

AWA 126286

Ionizing Potential Waves in Preionized Gases

R. F. FERNSLER

JAYCOR, Inc.
Alexandria, Virginia, 22303

March 14, 1983



NAVAL RESEARCH LABORATORY
Washington, D.C.

DTIC
SEL
APR 4 1983
S A D

Approved for public release; distribution unlimited.

DTIC FILE COPY

88 04 04 001

SECURITY CLASSIFICATION OF THIS PAGE (When Data Entered)

REPORT DOCUMENTATION PAGE		READ INSTRUCTIONS BEFORE COMPLETING FORM
1. REPORT NUMBER NRL Memorandum Report 5026	2. GOVT ACCESSION NO. AD-A126286	3. RECIPIENT'S CATALOG NUMBER
4. TITLE (and Subtitle) IONIZING POTENTIAL WAVES IN PREIONIZED GASES	5. TYPE OF REPORT & PERIOD COVERED Interim report on a continuing problem	
	6. PERFORMING ORG. REPORT NUMBER	
7. AUTHOR(s) R. F. Fernsler*	8. CONTRACT OR GRANT NUMBER(s)	
9. PERFORMING ORGANIZATION NAME AND ADDRESS Naval Research Laboratory Washington, DC 20375	10. PROGRAM ELEMENT, PROJECT, TASK AREA & WORK UNIT NUMBERS 61153N:RR011-09-41; 47-0871-0-2; and 62707E-0-OR40AA	
11. CONTROLLING OFFICE NAME AND ADDRESS Office of Naval Research Arlington, VA 22217 Defense Advanced Research Projects Agency Arlington, VA 22209 ATTN: Program Management/MIS	12. REPORT DATE March 14, 1983	
	13. NUMBER OF PAGES 26	
14. MONITORING AGENCY NAME & ADDRESS (if different from Controlling Office)	15. SECURITY CLASS. (of this report) UNCLASSIFIED	
	15a. DECLASSIFICATION/DOWNGRADING SCHEDULE	
16. DISTRIBUTION STATEMENT (of this Report) Approved for public release, distribution unlimited.		
17. DISTRIBUTION STATEMENT (of the abstract entered in Block 20, if different from Report)		
18. SUPPLEMENTARY NOTES Research supported by the Office of Naval Research and by the Defense Advanced Research Projects Agency (DoD) ARPA Order No. 4395 monitored by the Naval Surface Weapons Center under Contract N60921-82-WR-W0066. *Permanent address: JAYCOR - Alexandria, VA		
19. KEY WORDS (Continue on reverse side if necessary and identify by block number) Ionizing potential wave Electric breakdown Atmosphere Pre-ionized		
20. ABSTRACT (Continue on reverse side if necessary and identify by block number) A theory is presented to describe the advance of ionizing potential waves in preionized gases in nonuniform fields. The theory is based on the use of similarity and related arguments to bypass complicated mathematics and derive scaling relationships for wave speed as a function of applied potential and degree of ionization. For uniform preionization wave speed is predicted to scale linearly with applied potential and weaker than linearly with degree of preionization. These predictions are shown to agree well with recent potential-wave measurements obtained in electrical (Continued)		

DD FORM 1473
1 JAN 73

EDITION OF 1 NOV 68 IS OBSOLETE
S/N 0102-014-6601

SECURITY CLASSIFICATION OF THIS PAGE (When Data Entered)

SECURITY CLASSIFICATION OF THIS PAGE (When Data Entered)

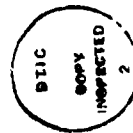
20. ABSTRACT (Continued)

discharge studies using lasers to preionize meter-long paths in atmospheric air. Modifications due to radially confined preionization, particle drift, and electrode and other effects are also discussed.

SECURITY CLASSIFICATION OF THIS PAGE (When Data Entered)

CONTENTS

1.	INTRODUCTION	1
2.	A SIMPLE SCALING MODEL	3
3.	WAVE EQUATIONS	3
4.	TRANSMISSION-LINE MODEL	5
5.	RADIALLY BOUNDED IPWs	11
6.	EXTENSION TO $\sigma_r \rightarrow 0$	12
7.	ADDITIONAL LIMITATIONS AND MODIFICATIONS	12
8.	DISCUSSION AND COMPARISON WITH EXPERIMENT	13
9.	CONCLUSION	14
10.	ACKNOWLEDGMENTS	16
11.	REFERENCES	16



A

IONIZING POTENTIAL WAVES IN PREIONIZED GASES

1. INTRODUCTION

As is well known, the application of a high potential across a pair of electrodes embedded in a weakly ionized gas causes waves of ionization to traverse the gas. Ionization occurs primarily at the advancing wave head where a high electric field heats existing electrons to temperatures sufficient for electron-impact ionization. Impact ionization rapidly raises the electron density, which is termed an electron avalanche, until the resulting wave conductivity becomes so large that space charge nullifies the local electric field. The wave thus converts field energy immediately ahead of the wave into gas ionization and excitation energy within the wave body.

The advance of a wave is governed by the interplay between the local electric field \underline{E} and the wave conductivity σ . \underline{E} determines the growth of σ due to electron-impact ionization while σ determines the evolution of \underline{E} via Maxwell's equations. An important parameter affecting wave propagation is the initial conductivity, σ_i , which exists immediately ahead of the wave. A number of mechanisms have been proposed for generating this conductivity in gases that are initially un-ionized. Among these mechanisms are: electron drift,¹⁻⁴ electron pressure,⁵ electron runaway,^{6,7} gas photoionization,⁸⁻¹³ and the photoelectric effect.¹⁴ The proponents of these different mechanisms all claim agreement with experiment, depending upon the interpretation of the experimental results.^{15,16}

In this paper we circumvent the controversy regarding the generation of σ_i by considering waves which propagate in preionized gases; here σ_i is specified as an initial condition. Such an analysis applies to all but the first ionizing wave propagating through a gas. The extension to propagation in un-ionized gases is also discussed.

We restrict the problem to nonuniform fields as illustrated in Fig. 1. At time zero an impulse voltage, ϕ_0 , is applied to a sharply contoured electrode. This voltage causes an ionizing potential wave (IPW) to emerge and propagate toward a distant ground. The fields far ahead of the wave are negligibly small. Our objective is to determine the propagation velocity, V , of the IPW as a function of ϕ_0 and σ_i .

Previous investigators have concentrated on determining the dependence of V on the initial electron density, n_{ei} , which is directly related to σ_i . Cravath and Loeb¹⁷ predicted a weak logarithmic dependence on n_{ei} . Schonland¹⁸ predicted that V scales as $n_{ei}^{1/3}$. Suzuki¹⁹ claimed, with some experimental justification, that V scales as $n_{ei}^{1/2}$. None of these theories indicates the dependence of V on electrode potential, ϕ_0 . Furthermore, all of the solutions presented for V depend upon one or more unknown variables. These variables, which include the wavefront thickness and the electron avalanche rate, may themselves depend upon n_{ei} [see also the criticisms of Winn²⁰ and Uman²¹].

The present paper attempts to remedy these shortcomings. Two objectives have been imposed on this attempt. The first is to obtain solutions which depend only on externally specified variables such as ϕ_0 and σ_i . Explicit dependence on the electron avalanche rate, for example, is considered unacceptable because this parameter can vary by orders of magnitude and a unique value cannot readily be chosen. The second objective is to emphasize the physical aspects of the problem, particularly with regard to

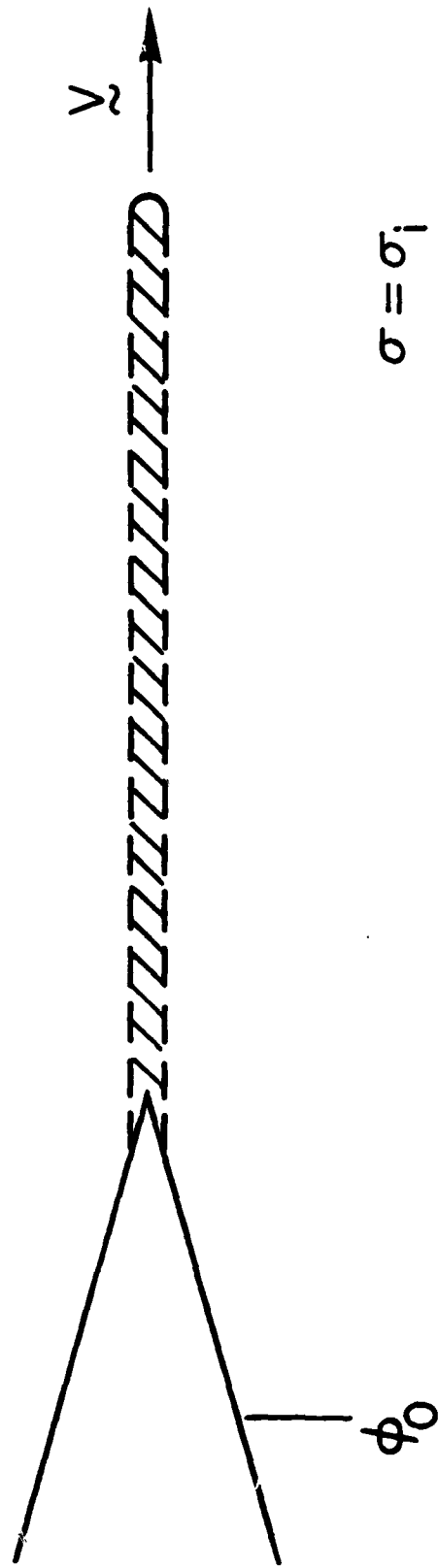


Fig. 1 — Schematic of an IPW. An electrode is held at constant voltage ϕ_0 . A filamentary IPW emerges and propagates with velocity V_z through a homogeneous preionized gas of conductivity σ_i . The conductivity inside the (shaded) IPW is large and approaches $\sigma_i \gg \sigma_i$.

obtaining scaling relationships. As a result, several solutions are actually presented. The first solution is essentially a dimensional argument which minimizes the mathematics. Subsequent solutions indicate limitations and modifications which arise in certain parameter regimes and applications.

2. A SIMPLE SCALING MODEL

Consider the basic problem. An electrode is held at constant voltage, ϕ_0 . A long filamentary IPW emanates from the electrode and propagates with velocity V through a homogeneous, weakly ionized gas of conductivity σ_i . We assume that V is determined solely by ϕ_0 and σ_i . Dimensional analysis then demands that

$$V = g_0 \phi_0 / 4\pi\sigma_i E_i \quad (1)$$

where $E_i(\phi_0, \sigma_i)$ is a characteristic field strength and g_0 is a numerical constant.

To determine $E_i(\phi_0, \sigma_i)$, we note that two principal rates govern the behavior of IPWs: $4\pi\sigma$ which controls the evolution of field \underline{E} ; and the electron avalanche rate, S , which controls the growth of conductivity σ . S is principally determined by E and, to a lesser extent, by the degree of ionization and excitation. For simplicity S is assumed to be a known function of E and σ , where wave conductivity σ is a measure of degree of ionization.

We can thus identify two characteristic rates: $4\pi\sigma_i$ and $S(E_i, \sigma_i)$. We presume that these two rates are related and set them equal to within a numerical coefficient, g_1 :

$$S(E_i, \sigma_i) = g_1 4\pi\sigma_i \quad (2)$$

This equation determines E_i for a given initial conductivity σ_i . Equation (1) then determines wave speed V . Estimates of g_0, g_1 are presented later.

To understand the physical origin of these relationships, imagine doubling all physical dimensions of the IPW shown in Fig. 1 while simultaneously doubling the electrode voltage ϕ_0 ; i.e., all characteristic lengths l_i become $2l_i$ while ϕ_0 becomes $2\phi_0$. This doubling redistributes but otherwise does not alter the local variables such as σ , S , and E (which scales as ϕ_0/l_i). Since the characteristic rates are unaltered while the characteristic lengths double, wave speed V which scales as $S l_i$ also doubles. We thus conclude that V scales linearly with ϕ_0 and that E_i in Eq. (1) is a function only of σ_i . The important point is that in the absence of geometrical constraints on length scales l_i , the initial conductivity σ_i determines the field E_i while the applied potential ϕ_0 controls the range over which E_i is distributed.

Equations (1) and (2) form the foundation of the present theory. What follows is an examination of more subtle issues. These include: (i) derive a solution based on a closed set of wave equations; (ii) identify and incorporate other wave parameters of interest; and (iii) determine when the model fails or needs modification.

3. WAVE EQUATIONS

We now present a more formal derivation of Eqs. (1) and (2) and assess some of their limitations. We express Maxwell's equations by

$$\underline{E} = -\underline{\nabla} \phi \quad (3)$$

and

$$\underline{\nabla} \cdot \left(\frac{\partial \underline{E}}{\partial t} + 4\pi\sigma \underline{E} \right) = 0 \quad (4)$$

where ϕ is the electrostatic potential. Ignoring electron diffusion and ignoring the massive and essentially immobile ions, the wave conductivity is given by

$$\sigma = en_e \mu \quad (5)$$

where e is the electron charge, n_e the electron density, and μ the electron mobility. The electron density evolves according to the continuity equation

$$\frac{\partial}{\partial t} n_e + \nabla \cdot (n_e \underline{u}) = S n_e \quad (6)$$

where \underline{u} is the electron fluid velocity and where the electron avalanche rate S equals the net electron production rate due to collisions. In the absence of electron diffusion, \underline{u} equals the electron drift velocity,

$$\underline{u} = -\mu \underline{E}. \quad (7)$$

Equations (3)-(7) are closed by specifying the avalanche rate S and mobility μ in terms of the field E , the conductivity σ , and the gas density N . On the time scales of interest we assume that N does not change so that S and μ are functions only of E and σ :

$$S = S(E, \sigma) \quad (8)$$

$$\mu = \mu(E, \sigma). \quad (9)$$

For a very weakly ionized wave the dependence on σ would also vanish; at higher degrees of ionization, processes such as electron-ion recombination and super-elastic collisions with excited molecules affect the electron dynamics, and thus affect the electron transport coefficients.

Equations (3)-(9) plus the appropriate boundary conditions determine the evolution of ionizing potential waves. To obtain stationary solutions in a wave frame traveling with constant velocity \underline{V} with respect to the laboratory (gas) frame, we use the traveling-wave condition,

$$\frac{\partial}{\partial t} = -\underline{V} \cdot \nabla \quad (10)$$

to rewrite Eqs. (4) and (5)-(7) as

$$\nabla \cdot ([\underline{V} \cdot \nabla] \underline{E} - 4\pi \sigma \underline{E}) = 0 \quad (11)$$

and

$$\nabla \cdot ([\underline{V} + \mu \underline{E}] \sigma / \mu) = -S \sigma / \mu. \quad (12)$$

To obtain scaling relationships, we look for self-similar solutions of the form

$$q(\underline{x}, t) = q_i f_q(\underline{\xi}) \quad (13)$$

where q is any variable, q_i is a characteristic value, and

$$\underline{\xi} = (\underline{x} - \underline{V}t) / l_i \quad (14)$$

with l_i being a characteristic length. The functions $f_q(\underline{\xi})$ are interrelated through the atomic-physics relationships (8) and (9) and through a dependence on σ_i , which characterizes the initial state of the gas. The functions do not depend on electrode potential ϕ_0 . Note that Eqs. (13) and (14) explicitly incorporate the traveling-wave condition (10).

Using the transformation

$$\nabla = l_i^{-1} \frac{\partial}{\partial \underline{\xi}}. \quad (15)$$

we reduce Eqs. (3), (11), and (12) to

$$E_r = \bar{C}_2 \phi_0 / l_r, \quad (16)$$

$$\frac{\partial}{\partial \xi} \cdot \left\{ \left[\frac{V}{l_r 4\pi\sigma_r} \right] \cdot \frac{\partial}{\partial \xi} \frac{\partial f_\phi}{\partial \xi} - f_\sigma \frac{\partial f_\phi}{\partial \xi} \right\} = 0, \quad (17)$$

and

$$\frac{\partial}{\partial \xi} \cdot \left\{ \left[\frac{V + \mu E}{l_r S_r} \right] \frac{f_\sigma}{f_\mu} \right\} = - \frac{f_\sigma f_S}{f_\mu} \quad (18)$$

where \bar{C}_2 is a dimensionless constant and where the characteristic avalanche rate is taken to be

$$S_r = S(E_r, \sigma_r). \quad (19)$$

Equations (16)-(19) preserve self-similarity provided the terms in square brackets are constant. This is valid provided Eqs. (1) and (2) are satisfied, and provided the electron drift velocity, $-\mu E$, is negligibly small. Since the electrostatic Eq. (3) is justified only when the wave speed is small compared with the speed of light, c , we expect Eqs. (1) and (2) to be valid only for

$$|\mu E_r| < V < c. \quad (20)$$

The self-similar analysis and Eqs. (1) and (2) become invalid at low wave speeds. This failure arises because the electrons, which are the dynamic particles controlling wave conductivity, are not stationary in the laboratory frame but are drifting with velocity $-\mu E$. The impact of this drift can be qualitatively understood by ignoring radial drift and assuming constant axial drift, $-\mu E_r$. Equations (17)-(19) then require that

$$S(E_r, \sigma_r) = g_1 4\pi\sigma_r (1 + \mu E_r / V). \quad (21a)$$

Or equivalently,

$$S(E_r, \sigma_r) - \frac{g_1}{g_0} \frac{E_r}{\phi_0} \mu E_r = g_1 4\pi\sigma_r, \quad (21b)$$

replacing Eq. (2). The latter equation demonstrates that E_r is in general determined by ϕ_0 as well as by σ_r . Furthermore, positive waves for which $\phi_0 > 0$ require a larger $|E_r|$ than negative waves for which $\phi_0 < 0$. According to Eq. (1), positive waves should therefore propagate slower. Indeed, Eq. (21a) rigorously restricts the negative-wave speed to $V > |\mu E_r|$, which reflects the fact that a wave cannot propagate more slowly than its constituent particles. A similar restriction applies to positive waves only if $S(E_r, \sigma_r)$ increases no faster than linearly with E_r .

This section has provided a formal basis for the IPW velocity solution, $V(\phi_0, \sigma_r)$, presented earlier. The range of applicability has also been discussed. The next section takes yet a different approach, discusses additional limitations, and provides estimates for the coefficients g_0 , g_1 , and \bar{C}_2 .

4. TRANSMISSION-LINE MODEL

To simplify the problem further, we use a transmission-line analysis to approximate Maxwell's equations. The electric field along the axis of propagation is then given by

$$E = - \frac{\partial \phi}{\partial z} - \frac{\partial}{\partial t} (L_z I) \quad (22)$$

where the last term allows for inductive corrections. Ohm's law relates the current I to the wave conductance Σ via

$$I = \Sigma E \quad (23)$$

where Σ equals a radial integral of wave conductivity, σ . Equation (12) yields

$$-\frac{\partial}{\partial z} [(V + \mu E) \Sigma / \mu] = \bar{S} \Sigma / \mu \quad (24)$$

where \bar{S} is a radial average of S .

Charge conservation produces

$$\frac{\partial}{\partial t} (C_z \phi) + \frac{\partial I}{\partial z} = 0 \quad (25)$$

where $C_z \phi$ is the space charge distributed per unit length along the wave. The distributed capacitance C_z and inductance L_z satisfy

$$(L_z C_z)^{-1/2} \leq c. \quad (26)$$

We assume for convenience that $(L_z C_z)$ is constant and use the traveling-wave condition (10) to obtain

$$E = -\frac{\partial \phi}{\partial z} (1 - V^2 L_z C_z) \quad (27)$$

$$I = V C_z \phi = \Sigma E \quad (28)$$

and

$$-\frac{\partial}{\partial z} \ln (\mu E) = \frac{C_z (V + \mu E)}{\Sigma (1 - V^2 L_z C_z)} - \frac{V + \mu E}{V} \frac{\partial}{\partial z} \ln C_z - \frac{\bar{S}}{V}. \quad (29)$$

Equations (26)-(29) demonstrate that inductive effects serve principally to limit the wave speed to

$$V < (L_z C_z)^{-1/2} \leq c. \quad (30)$$

Henceforth we generally ignore inductive effects except to impose constraint (30).

Let us use Eqs. (24) and (29) to describe the qualitative structure of IPWs. Well within the wave the conductance Σ approaches its maximum value, Σ_f , while the field E approaches a low value, E_f . E_f is a maintenance field defined by the condition

$$\bar{S}(E_f, \sigma_f) = 0 \quad (31)$$

where σ_f is the final conductivity attained in the wave body. If σ_f were zero, E_f would equal the breakdown field, E_b ; for large σ_f , E_f can be well below E_b due to the ionization and electron heating provided by the excited molecules.

Approaching the head of the wave, E and \bar{S} begin to rise while Σ gradually falls. As \bar{S} becomes large, the fall of Σ accelerates. As a result, E and \bar{S} attain peak values, E_r and \bar{S}_r , respectively, at the wave tip. Beyond the tip E and \bar{S} approach zero. In this region the distributed space charge, $C_z \phi$, and capacitance, C_z , also approach zero.

The transmission-line equations are incomplete since the wave radius, r_w , and the axial dependence of C_z are unknown. We thus supplement these equations by modeling the IPW as a long, space-charged filament. Electrostatics then dictates that axial variations in the wave head are characterized by a common length scale,

$$l_r = \bar{C}_z \phi_r / E_r \quad (32)$$

where \bar{C}_2 and ϕ_0 characterize the capacitance and potential, respectively, of the wave head. Typically, $\bar{C}_2 \approx 0.2$ in Gaussian units. Note that a common length scale can be imposed only if condition (20) is satisfied. See Appendix A for details.

We express the tip conductance by

$$\Sigma_t = g' \sigma_t \pi r_w^2 \quad (33)$$

and set the wave radius to

$$r_w = g'' l_t \quad (34)$$

The strong dependence of the avalanche rate S and weak dependence of the mobility μ on field E suggests that $g' \approx 1$ and $g'' < 1$.

Inserting these assumptions into Eqs. (24) and (29) and imposing constraint (20) yields, as outlined in Appendix A,

$$V = g_0 \phi_t 4\pi\sigma_t / E_t \quad (35)$$

and

$$S(E_t, \sigma_t) \approx \bar{S}_t = g_1 4\pi\sigma_t \quad (36)$$

where

$$g_0 = g'(g''\bar{C}_2)^2 / 4C_{zt} \quad (37)$$

and

$$g_1 = g_0 / \bar{C}_2 \quad (38)$$

Here the capacitance at the wave tip satisfies $C_{zt} \ll \bar{C}_2$.

Equation (35) is equivalent to Eq. (1) provided the tip potential ϕ_t equals the electrode potential ϕ_0 . This equivalence is justified, to order $\bar{C}_2 \ll 1$, provided the resistive voltage drop within the wave body is small. This proviso is also required to justify the assumption of constant velocity V . A generally sufficient condition is that the IPW length satisfies

$$l \ll l_{\max} = \phi_0 / E_f \quad (39)$$

where l_{\max} is the nominal maximum propagation distance. We point out that IPWs can actually propagate, with diminishing velocity, for distances further than l_{\max} due to the space charge stored in the wave body. This charge and the capacitive structure of IPWs permits propagation for several "RC" times, suggesting that distances up to $3l_{\max}$ may be possible. This feature additionally explains the ability of IPWs to continue propagating even if the electrode voltage is suddenly terminated.²²

The transmission-line analysis and electrostatic model have reproduced the original solutions given by Eqs. (1) and (2). We now use these models to estimate the coefficients g_0 and g_1 .

Equation (35) has a simple physical basis. An IPW propagates by transforming conduction current in the wave body into displacement current at the wave tip. This transformation produces high space-charge fields at the tip which generate high conductivity in the body. Conduction currents are negligible at the tip only if the electric field rises to its peak value E_t in a short distance

$$l_t \ll V / 4\pi\sigma_t \quad (40)$$

Equation (32) converts this condition into

$$V \gg \bar{C}_2 \phi_t 4\pi\sigma_t / E_t \quad (41)$$

The strength of this inequality is limited by the fact that conduction currents dominate inside the wave. Hence, Eqs. (35), (38), and (41) suggest that

$$g_0 \approx 10 \bar{C}_2 \approx 2 \quad (42)$$

and

$$g_1 \approx 10. \quad (43)$$

To illustrate these findings, consider very weakly preionized air of density N . The reduced avalanche rate, S/N , is then well known²³⁻²⁵ as a function of reduced field, E/N , as shown in Fig. 2. A corresponding plot of V/ϕ_0 as a function of σ_i/N is shown in Fig. 3. The latter plot is based on Eqs. (1), (2), (42), and (43). Also plotted in Fig. 3 is the electron drift speed, $|\mu E_i|$, which is presumed small compared with wave speed V .

Several features of these plots are noteworthy. First, as σ_i/N becomes small E_i approaches E_b , where the breakdown strength $E_b/N \approx 100$ Td in air. [A Townsend (Td) equals 10^{-17} Volts-cm² \approx 0.33 Volts/cm-torr.] As a result V/ϕ_0 scales nearly linearly with σ_i/N . This dependence lessens at high σ_i/N . At $\sigma_i/N \geq 10^{-10}$ cm³/sec, V/ϕ_0 is essentially constant. Here S approaches S_{\max} which is the maximum possible ionization rate in the gas. In very weakly preionized air, $S_{\max}/N \approx 5 \times 10^{-8}$ cm³/sec.

The restriction on avalanche rate S indicates that relationship (2) is valid only for

$$\sigma_i < \sigma_{\max} \equiv S_{\max}/4\pi g_1. \quad (44)$$

Above this limit conduction currents ahead of the wave redistribute the wave space charge and associated fields before the conductivity can avalanche. We thus conclude that unbounded traveling-wave solutions cease to exist at high σ_i . This failure is closely related to the energy arguments of Appendix B which show that

$$V/\phi_0 < 5 \times 10^5 \text{ cm/Volt-sec.}$$

A different failure arises at low σ_i where E_i approaches E_b . Here electron attachment generates large numbers of negative ions and ion currents which can short-circuit the electron avalanche process. We express the avalanche rate as

$$S = (\alpha - \eta) \mu E \quad (45)$$

where $\alpha \mu E$ is the electron-impact ionization rate and $\eta \mu E$ is the net electron-attachment rate; α is termed the first Townsend coefficient and η the attachment coefficient. Ion currents can be ignored provided the production of negative ions due to electron attachment does not exceed the production of electrons. We thus require that the peak avalanche rate satisfies

$$S_i > \eta(E_i) \mu E_i \quad (46)$$

and hence that

$$\sigma_i > \sigma_{\min} \equiv \eta(E_b) \mu E_b / 4\pi g_1 \quad (47)$$

where the breakdown field E_b is defined by

$$\alpha(E_b) = \eta(E_b). \quad (48)$$

We identify σ_{\min} as the minimum initial (electron) conductivity required to augment IPW propagation.

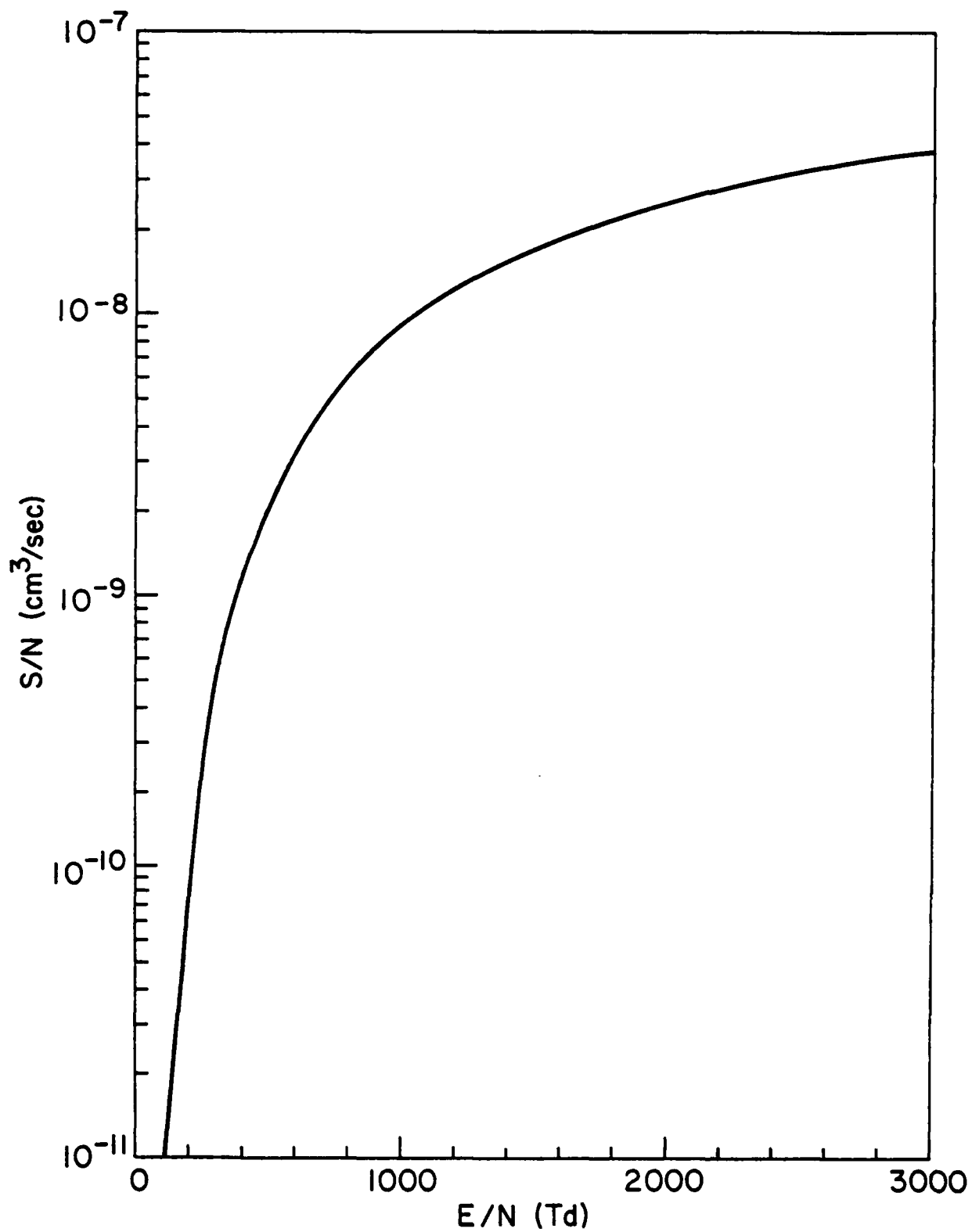


Fig. 2 — Electron impact ionization rate, S , as a function of field strength, E , in weakly ionized air of density of N .

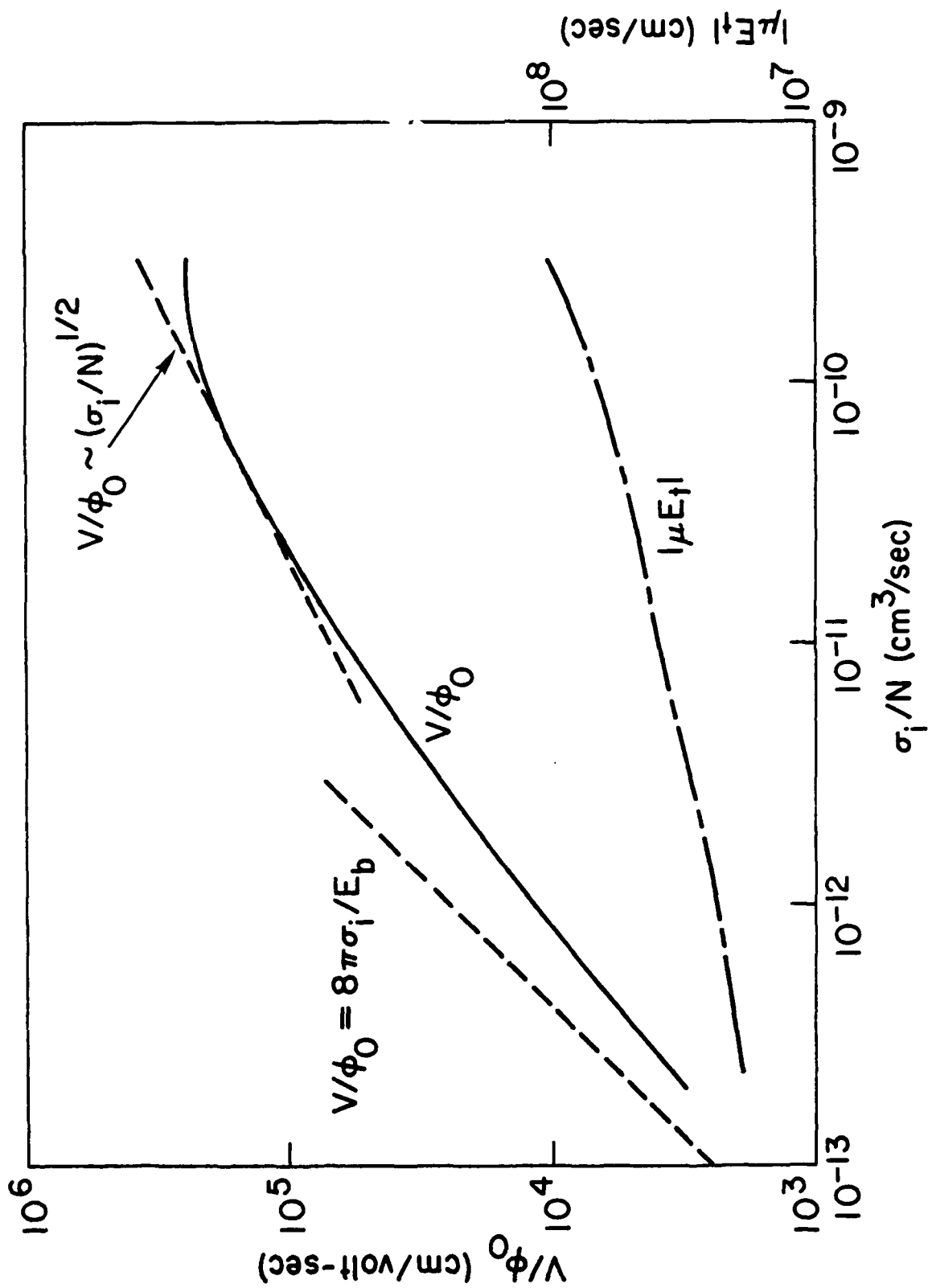


Fig. 3 - Scaling of IPW velocity V as a function of initial conductivity σ_i in weakly preionized air of density N . ϕ_0 is the applied potential. Also plotted is the electron drift speed, $|\mu E_{\perp}|$, which is presumed small compared with V .

In cold weakly preionized air, $\eta(E_b)/N \approx 1.5 \times 10^{-19} \text{ cm}^2$ and $\mu E_b \approx 1.5 \times 10^7 \text{ cm/sec}$. Assuming $g_1 = 10$, conditions (44) and (47) reduce to

$$10^{-14} < \frac{\sigma_i}{N} < 5 \times 10^{-10} \text{ cm}^3/\text{sec}. \quad (49)$$

Because σ_i scales as the degree of preionization, n_{ei}/N , the lower limit is generally more important at high N while the upper limit is more important at low N .

5. RADIALLY BOUNDED IPWs

In the preceding theory the wave radius r_w was determined by ϕ_0 and σ_i . We now consider the modifications which arise if r_w is externally constrained, either by the presence of walls or by the initial profile of σ_i . We term these waves radially bounded.

Radial constraints have two main effects. The first is that the internal wave structure is altered so that a single axial length no longer characterizes Σ , E , and C_z . In particular, the distributed capacitance C_z (rather than potential ϕ) varies slowly throughout the wave head and may be treated as constant. Setting $C_z = \bar{C}_z$ and evaluating Eqs. (29) and (33) at the peak field E_i yields

$$V = g_2 (4\pi\sigma_i \bar{S}_i)^{1/2} r_b \quad (50)$$

where r_b is the bounded-wave radius and

$$g_2^2 = \frac{g_1}{4\bar{C}_z} \frac{1 - V^2 L_z C_z}{1 + \mu E_i/V} \approx 1. \quad (51)$$

A nearly identical equation was obtained by Suzuki.¹⁹

The second effect is that E_i is determined not by the initial conductivity but by

$$E_i = g'' \bar{C}_z \phi_0 / r_b, \quad (52)$$

provided the resistive voltage drop in the wave body is negligible. This equation is a direct extension of Eqs. (32) and (34) and closes the velocity solution of Eq. (50) by defining the peak avalanche rate,

$$\bar{S}_i \approx S(E_i, \sigma_i). \quad (53)$$

The transition from the unbounded wave solutions, given by Eqs. (1) and (2), to the bounded solutions, given by Eqs. (50)-(53), occurs when the bounded wave radius r_b becomes less than the unbounded radius. This transition typically occurs in air when

$$\phi_0 / r_b N \geq 10^{-13} \text{ Volt-cm}^2. \quad (54)$$

The character of radially bounded IPWs differs from that of unbounded IPWs. Bounded IPWs are predicted to behave as follows: wave speed V scales nearly linearly with $\sigma_i^{1/2}$; V exhibits a monotonic but generally nonlinear dependence on ϕ_0 ; V exhibits a nonmonotonic dependence on bounded-wave radius r_b and on gas density N . Moreover, constraints (44) and (47) on σ_i are no longer valid since Eq. (2) does not apply. In particular, bounded-wave solutions exist even at high $\sigma_i \gg \sigma_{\max}$. The reason is that bounded waves are constrained to be filamentary which is the characteristic required for space-charge field enhancement; i.e., the absence of conductivity outside r_b ensures that space-charge fields and subsequent avalanching will develop inside r_b .

6. EXTENSION TO $\sigma_i \rightarrow 0$

For many problems of interest the initial conductivity ahead of the wave is well below the value, σ_{\min} , required to influence IPW propagation. Waves can still propagate, however, provided the wave itself can generate the necessary seed ionization at the wave tip.

The only mechanism explicitly incorporated in the theory for generating this seed ionization is electron drift. Here the directed motion of the electrons due to the local electric field advances the wave. Equation (29) indicates that for vanishing tip conductance, wave speed V approaches

$$V = -\mu E_t. \quad (55)$$

This is positive definite only for negative waves where $\underline{V} \cdot \underline{E} < 0$. Electron drift can thus account for slow negative waves but cannot account for fast ($V \gg 10^8$ cm/sec) negative waves or for positive waves.

The theory can easily accommodate other seed ionization mechanisms provided the tip conductivity or conductance can be estimated. The only formal constraint is that condition (47) be satisfied. A less formal constraint is that the seed mechanism account for positive waves as well as negative waves since the experimental character of both waves is so similar. This last constraint excludes, for example, the electron-runaway mechanism.^{6,7}

Two proposed mechanisms in nonuniform fields are gas photoionization^{3,13} and electron pressure.⁵ (The photoelectric effect¹⁴ is presumed irrelevant because the ground electrode is in a weak-field region far from the wave.) For positive waves the electron-pressure mechanism requires an anomalous electron-heating process which so heats electrons in the positive wavefront that the electron fluid velocity reverses direction and opposes electron drift. Such a reversal is deemed improbable because these electrons would then rapidly lose energy to the electric field rather than gain it.

A major criticism of the photoionization mechanism is that the relevant atomic physics is often unknown.^{14,26} Photoionization nonetheless remains promising because: (i) ample experimental evidence²⁷ demonstrates that it or a similar process occurs in electrical discharges and, by inference, occurs in IPWs; and (ii) inclusion of the experimentally determined photoionization rate in the electron continuity equation directly leads to fast positive and negative waves.^{12,13}

To illustrate the role of seed ionization mechanisms on wave propagation, consider gas photoionization. Ionizing photons are created within the wave with an efficiency δ per electron-impact ionization event. The photon-production process determines whether δ depends on gas density N , field parameter E/N , or degree of ionization. Typically, $\delta \ll 1$.⁸ Such a low efficiency means that photoionization is unimportant in the wave head or body.

Photoionization can nonetheless be important ahead of the wave provided the photon-absorption length, λ_a , is much longer than the characteristic electron transport lengths. Photoionization then generates, within a length λ_a outside the wave head, an initial conductivity of $\sigma_i \approx \delta \sigma_f$ where σ_f is the final wave conductivity. This seed ionization is sufficient to sustain wave propagation provided the gain in conductivity, σ_f/σ_i , due to electron-impact ionization in the wave head exceeds δ^{-1} . See Ref. 28 for further discussion.

7. ADDITIONAL LIMITATIONS AND MODIFICATIONS

Two additional parameters which can affect V and thereby invalidate or modify the theory are electrode effects and a finite rise-time, τ_r , of the applied voltage. Only if

$$\tau_r \ll l_{\max}/V \quad (56)$$

can the voltage rise-time be ignored. If this condition is not satisfied, the effective electrode voltage is reduced and Eq. (1) should be adjusted accordingly. Alternatively if ϕ_0 rises linearly with time, wave speed is ultimately given from Eqs. (10) and (27) by

$$V = E_f^{-1} \frac{d\phi_0}{dt} (1 - V^2 L_2 C_2) \quad (57)$$

where the asymptotic field strength E_f is defined by Eq. (31).

Electrode effects assume a particular importance when examining the differences between positive and negative waves. Positive waves generate an electron flux that flows into the electrode, whereas negative waves require an electron flux that emanates from the electrode. Negative waves thus require an active electron-emitting surface whereas positive waves require an essentially inactive, electron-absorbing surface. Any restriction on electron current flowing in or out of the electrode results in resistive sheaths, which reduce the voltage appearing at the wave head and thereby reduce wave speed V . Electrode sheath restrictions are thus usually more severe for negative waves than for positive waves. Such restrictions and differences become unimportant, however, when the applied potential is large (typically, $\phi_0 > 10$ kV) compared with the sheath potential.

8. DISCUSSION AND COMPARISON WITH EXPERIMENT

Let us briefly review the previous theoretical predictions. We have identified two types of waves: radially bounded and radially unbounded. Unbounded means that the wave radius is smaller than any external constraint. The velocity of unbounded waves is predicted to scale at low σ_i/N as

$$V \sim \phi_0 \sigma_i / N \sim \phi_0 n_{ei} / N^2 \quad (58)$$

where N is the gas density and n_{ei} is the initial electron density ahead of the wave. By contrast, the velocity of radially bounded waves is predicted to scale as $\sigma_i^{1/2}$ and to depend in a complicated manner on ϕ_0 , N , and bounded-wave radius r_b . At high ϕ_0 and low N , r_b this dependence simplifies to

$$V \sim (\sigma_i N)^{1/2} r_b \sim n_{ei}^{1/2} r_b. \quad (59)$$

Electrode effects and other processes can easily modify these scalings.

Corresponding to the two types of waves are two classes of experiments: IPWs launched in low-pressure glow discharges where the initial conductivity is determined by the glow-discharge current; and high-pressure experiments using lasers to preionize the gas. A third pertinent category is the long spark²⁹ in which a succession of IPWs (streamers, leaders, and return strokes) propagate along the same path. A difficulty with the latter experiments is that the state of the gas between successive waves is unknown, and hence σ_i is indeterminate. We point out that each successive wave encounters an initial conductivity much higher than that experienced by its predecessor. As a result wave speed is higher and wave radius is (slightly) smaller. Successive IPWs are therefore predicted to be radially unbounded provided the predecessor is (until σ_i exceeds σ_{\max} as defined by Eq. (44)).

We focus on a limited subset of the available experimental data. Consider first the laser-guided discharges of Koopman and Saum³⁰ and of Greig, et al.^{31,32} These experiments used a pulse of energy from a Nd: glass laser or a CO₂ laser to preionize meter-long paths in atmospheric air. The subsequent application of an impulse voltage across electrodes at each end induced IPWs to propagate within the laser-formed channel, ultimately leading to a high-current discharge. The initial conductivity was controlled by varying either the laser energy or the delay time between firing the laser and applying the impulse voltage.

The minimum laser-generated electron conductivity, σ_{\min} , required to guide IPWs was consistent with predictions (47) and (49). Analysis of the experiments indicated that thermal detachment of negative ions by laser-heated molecules,^{31,32} rather than photodetachment by IPW photons,³⁰ played a key role in determining σ_{\min} .

The experiments of Greig, et al. attempted to determine the dependence of wave speed V on initial conductivity σ_i and electrode voltage ϕ_0 . Wave speed was determined by measuring the arrival time of the potential wave at several axial positions along the laser-designated path using capacitive voltage probes. Results for V as a function of ϕ_0 are shown in Fig. 4 for an initial conductivity of $\sigma_i/N \approx 10^{-12}$ cm³/sec. Not only is the plot linear, but the measured value of $V/\phi_0 \approx 5 \times 10^3$ cm/Volt-sec agrees to within experimental uncertainty (a factor of 2 or more for σ_i/N) with that predicted by Fig. 3. Such agreement is remarkable considering the order-of-magnitude estimates used for coefficients g_0 and g_1 . The dependence of V on σ_i was less clear due to a large scatter in the conductivity measurements. V was shown, however, to exhibit a strong monotonic dependence on σ_i .

Several other features of Greig's experiments are noteworthy. First, optical diagnostics indicated that the IPWs were radially unbounded since the wave radius ($r_w \leq 0.1$ cm) was smaller than the radius (0.2 to 2 cm) of the laser-formed channels. Second, the guidance afforded by the laser preionization was strong; IPWs could be guided, for example, even along laser paths that were perpendicular to the static electric field lines. This plus the large increase in guided wave speed over unguided wave speed again supports the prediction that σ_i strongly influences wave propagation. Third, wave speed and wave potential decreased with increasing propagation length, l . And fourth, the maximum propagation length for a given electrode potential ϕ_0 corresponded to an average electric field (ϕ_0/l) of

$$E_{\min} \approx 1.5 \text{ kV/cm.} \quad (60)$$

This field is roughly one third of the maintenance field, E_f , predicted by numerical simulations based on the detailed air chemistry code, CHMAIR.³³ These simulations assumed that laser preheating raised the channel temperature from 300°K to 800°K and lowered the gas density accordingly.³² The many approximations employed in the simulations preclude an accurate determination of E_f . The results nonetheless support the earlier contention that E_{\min} could be as low as one third of E_f due to the capacitive structure of IPWs.

We now consider IPWs launched in low-pressure glow discharges where the wave radius is typically restricted to the glow-discharge radius. A review of these and related experiments was given by Fowler.³⁴ We shall concentrate, however, on the more recent experiments of Suzuki.¹⁹ The latter work is selected because it specifies all primary parameters of interest. Suzuki additionally presented a bounded-wave theory similar to that given here.

Suzuki's results may be summarized as follows: wave speed V scaled as $n_{ei}^{1/2}$; V exhibited a monotonic dependence on ϕ_0 which saturated at high ϕ_0 ; V scaled linearly with ϕ_0/τ_r , where τ_r is the voltage rise-time; and positive waves typically propagated faster than negative waves. These findings agree well with the bounded-wave predictions. This agreement was further confirmed by numerical simulations which coupled the chemistry code CHMAIR to Eqs. (27) and (29), using constant specified wave speed V and a constant capacitance of $C_2 = 0.2$.

9. CONCLUSION

In this paper we have concentrated on the propagation of ionizing waves in preionized gases. We have shown that these waves propagate not because of directed-particle motion, but because electron-impact ionization due to the local electric field raises the degree of ionization and hence the conductivity in the wave head. As a result the wave space charge and fields are displaced forward, thereby causing ionization to commence in a new region ahead of the wave. Processes such as electron drift, diffusion, etc. are of secondary or lesser importance.

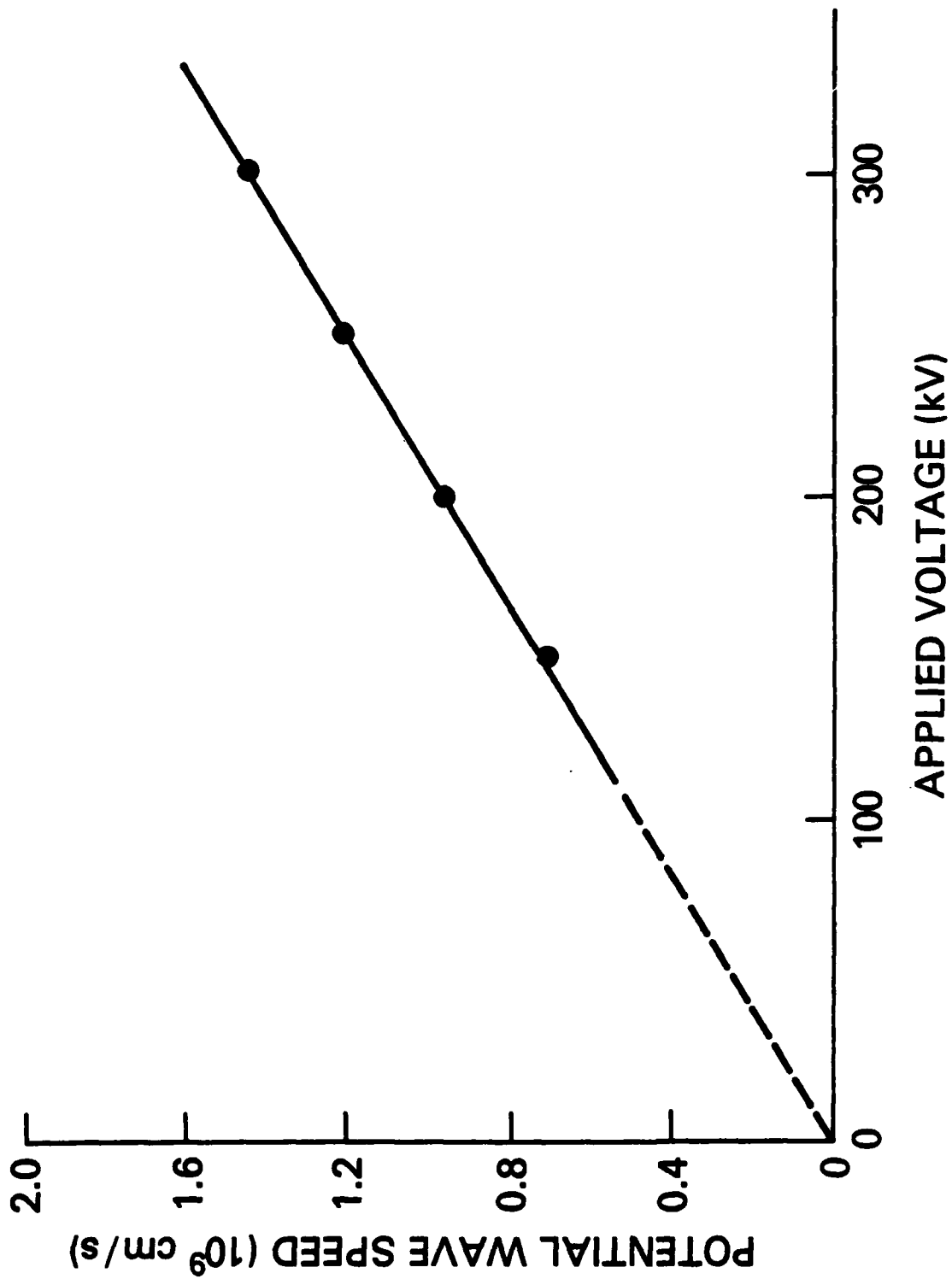


Fig. 4 — Potential wave velocity as a function of applied voltage as measured by Greig et al.¹² for laser-guided discharges in air

The crux of the analysis has been the use of similarity and related arguments to by-pass the mathematical complexities and arrive at a wave velocity, $V(\phi_0, \sigma_i)$. The complexities chiefly comprise two forms: the two-dimensional elliptic character of Maxwell's equations, a feature which is responsible for space-charge field enhancement and is thus essential for wave propagation in nonuniform fields; and complications due to the functional dependencies of S and μ on E , N , and σ . The similarity argument is like that used in simple thermodynamic and hydrodynamic problems.^{35,36} It is based on the fact that the continuity equation for conductivity σ and Maxwell's equations for field \underline{E} and potential ϕ are linear.

In the simplest nonuniform field problem, we have found that wave speed scales nearly linearly with the external control parameters σ_i and ϕ_0 . We have also discussed the influence of constraints such as radial boundaries and electrode effects, and have outlined how to extend the analysis to propagation in un-ionized gases. Comparison with experiment has generally been favorable. Agreement between theory and experiment at a few operating points is insufficient, however, to validate a theory, as evidenced by the wealth of IPW theories and good agreement claimed for all. Of greater use is the determination and evaluation of scaling relationships between measurable variables. Until careful measurements such as those of Suzuki¹⁹ have been performed over a wide parameter space, distinctions between differing theories will likely remain unresolved.

10. ACKNOWLEDGMENTS

The author wishes to express his appreciation to Dr. M. Raleigh for a careful reading of the manuscript, to Dr. R. E. Pechacek for patiently explaining the experimental measurements, and to Dr. J. R. Greig for useful discussions and encouragement. This work was supported by the Office of Naval Research and by the Defense Advanced Research Projects Agency.

11. REFERENCES

1. F. Llewellyn-Jones, *Ionization and Breakdown in Gases* (Methuen, London, 1966), p. 50.
2. N.W. Albright and D.A. Tidman, *Phys. Fluids* **15**, 86 (1972).
3. A.L. Ward, *Phys. Rev. A* **138**, 1357 (1965).
4. A.J. Davies, C.S. Davies, and C.J. Evans, *Proc. IEE* **118**, 816 (1971).
5. R.G. Fowler, *Advances in Electronics and Electron Physics* **41**, 1 (1976).
6. L.P. Babich and Yu. L. Stankevich, *Zh. Tekh. Fiz.* **42**, 1669 (1972) [*Sov. Phys. Tech. Phys.* **17**, 1333 (1973)].
7. E.E. Kunhardt and W.W. Byszewski, *Phys. Rev. A* **21**, 2069 (1980).
8. H. Raether, *Electron Avalanches and Breakdown in Gases*, (Butterworth, London, 1964).
9. J.M. Meek, *Phys. Rev.* **57**, 722 (1940).
10. R. Klingbeil, D.A. Tidman, and R.F. Fernsler, *Phys. Fluids* **15**, 1969 (1972).
11. E.D. Lozansky and O.B. Firsov, *J. Phys.* **D6**, 976 (1973).
12. L.E. Kline and J.G. Siambis, *Phys. Rev. A* **5**, 794 (1972).

13. K. Yoshida and H. Tagashira, *J. Phys.* **D9**, 491 (1976).
14. J. Dutton, S.C. Haydon, and F. Llewellyn-Jones, *Proc. Roy. Soc. (London)* **A218**, 206 (1953).
15. F.R. Dickey, *J. Appl. Phys.* **23**, 1336 (1952).
16. E.E. Kunhardt, *IEEE Trans. Plasma Sci.* **8**, 130 (1980).
17. A.M. Cravath and L.B. Loeb, *Phys.* **6**, 125 (1935).
18. B.F.J. Schonland, *Proc. Roy. Soc. (London)* **A164**, 132 (1938).
19. T. Suzuki, *J. Appl. Phys.* **48**, 5001 (1977).
20. W.P. Winn, *J. Geophys. Res.* **70**, 3265 (1965).
21. M.A. Uman, *Lightning* (McGraw-Hill, New York, 1969), p. 223.
22. N.S. Rudenko and V.I. Smetanin, *Zh. Tekh. Fiz.* **44**, 2602 (1974) [*Sov. Phys. Tech. Phys.* **19**, 1616 (1975)].
23. C.R. Rao and G.R.G. Raju, *J. Phys.* **D4**, 494 (1971).
24. M.A. Harrison and R. Geballe, *Phys. Rev.* **91**, 1 (1953).
25. H. Ryzko, *Proc. Phys. Soc. London* **85**, 1283, 1965.
26. F. Llewellyn-Jones, *Hand. Phys.* **22**, pp. 28-47 (1956).
27. G.W. Penney and G.T. Hummert, *J. Appl. Phys.* **41**, 572 (1970).
28. L.B. Loeb, *Hand. Phys.* **22**, p. 488 (1956).
29. G.N. Aleksandrov, B.N. Gorin, V.P. Redkov, I.S. Stekol'nikov, and A.V. Shkilev, *Dokl. Akad. Nauk SSSR* **183**, 1048 (1968) [*Sov. Phys.-Dokl.* **13**, 1246 (1969)].
30. D.W. Koopman and K.A. Saum, *J. Appl. Phys.* **44**, 5328 (1973).
31. J.R. Greig, D.W. Koopman, R.F. Fernsler, R.E. Pechacek, I.M. Vitkovitsky, and A.W. Ali, *Phys. Rev. Lett.* **41**, 174 (1978).
32. R. Fernsler, J.R. Greig, J. Halle, R. Pechacek, M. Raleigh, and I.M. Vitkovitsky, AIAA-80-1380 (1980). Also, R. E. Pechacek (private communication, Fig. 4).
33. R.F. Fernsler, A.W. Ali, J.R. Greig, and I.M. Vitkovitsky, *Bull. Amer. Phys. Soc.* **23**, 775 (1978) [*Naval Research Laboratory MR4110* (1979)].
34. R.G. Fowler, *Advances in Electronics and Electron Physics* **35**, 1 (1974).
35. G.K. Batchelor, *An Introduction to Fluid Dynamics* (Cambridge University Press, Cambridge, 1967), p. 188.

36. Ya. B. Zel'dovich and Yu. P. Raizer, *Physics of Shock Waves and High-Temperature Hydrodynamic Phenomena*, Vol. i (Academic, New York, 1966), pp. 93-95.
37. A. Haberstick, thesis. University of Maryland, 1964.
38. W.P. Winn, *J. Appl. Phys.* **38**, 783 (1967).

Appendix A
CHARACTERISTIC LENGTH SCALES

Consider the following length scales which are to be evaluated at the peak field, E_r :

$$l_1 = \left| \frac{\partial}{\partial z} \ln \Sigma \right|^{-1} \quad (\text{A1})$$

$$l_2 = \left| \frac{\partial}{\partial z} \ln C_2 \right|^{-1} \quad (\text{A2})$$

$$l_3 = \left| \frac{\partial}{\partial z} \ln (C_2 \phi) \right|^{-1} \quad (\text{A3})$$

$$l_4 = \left| \frac{\partial^2}{\partial z^2} \ln C_2 \right|^{-1/2} \quad (\text{A4})$$

$$l_5 = \left| \frac{\partial^2}{\partial z^2} \ln (\mu E) \right|^{-1/2} \quad (\text{A5})$$

where by definition

$$\left. \frac{\partial}{\partial z} E \right|_{E_r} = 0. \quad (\text{A6})$$

We employ the reasonable assumption that the mobility μ and avalanche rate \bar{S} also attain peak values at E_r . Hence, at E_r

$$\left. \frac{\partial}{\partial z} (\bar{S}, \mu) \right|_{E_r} = 0 \quad (\text{A7})$$

and

$$\left| \frac{\partial}{\partial z} \ln (\Sigma/\mu) \right|^{-1} = l_1. \quad (\text{A8})$$

Evaluating Eqs. (24) and (28) at E_r then yields

$$V + \mu E_r = \bar{S}_r l_1 \quad (\text{A9})$$

$$V = \Sigma_r E_r / C_{2r} \phi_r. \quad (\text{A10})$$

Substituting these results into Eq. (29) evaluated at E_r produces

$$\frac{1}{l_1} - \frac{1}{l_2} = \frac{1}{l_6} \quad (\text{A11})$$

where

$$l_6 = \frac{\phi_r}{E_r} (1 - V^2 L_2 C_2). \quad (\text{A12})$$

Similar manipulations performed on the first derivatives of Eqs. (24), (28), and (29) lead to

$$l_3 = l_1 \quad (\text{A13})$$

and

$$\left(\frac{1}{1 + \mu E_t / V} \right) \frac{1}{l_5^2} - \frac{1}{l_3^2} = \frac{1}{l_6^2}. \quad (\text{A14})$$

The dependence of the length scales l_i on wave speed V in Eqs. (A11)-(A14) vanishes in the limit

$$|\mu E_t| \ll V \ll (L_2 C_2)^{-1/2}. \quad (\text{A15})$$

Hence, by imposing this constraint we can neglect wave motion and simply consider the electrostatic problem.

For a filamentary wave in which the radius r_w and body length l satisfy

$$r_w < l_3 < l. \quad (\text{A16})$$

as is implicitly assumed in the transmission-line equations, Gauss's law dictates that the electrostatic field near the tip of the wave is determined by the distribution of space charge in the wave head. Since the mobility μ is not a strong function of field E , we thus expect that

$$l_5 \approx l_3 \approx l_t \quad (\text{A17})$$

where

$$l_t = \bar{C}_z \phi_t / E_t. \quad (\text{A18})$$

Here $\bar{C}_z \phi_t$ characterizes the space charge in the wave head, and E_t is the peak field at the tip. In the absence of coaxial ground returns, the distributed capacitance is given in Gaussian units by

$$\bar{C}_z \approx [2 \ln(2l_3/r_w)]^{-1} \quad (\text{A19})$$

and typically satisfies

$$\bar{C}_z \approx 0.2. \quad (\text{A20})$$

Combining Eqs. (A11)-(A15) with Eqs. (A17), (A18), and (A20) produces the desired result that

$$l_i \approx l_t < l_6 \quad (\text{A21})$$

for $i = 1, 5$.

We use result (A21) as follows. Eliminating wave speed V from Eqs. (A9) and (A10) produces, to order $\mu E_t / V$,

$$\bar{S}_t \approx \frac{\Sigma_t E_t}{C_{zt} \phi_t} \frac{1}{l_t} = \frac{\bar{C}_z}{C_{zt}} \frac{\Sigma_t}{l_t^2}. \quad (\text{A22})$$

Substituting Eqs. (33) and (34) into Eqs. (A9) and (A22) then leads directly to the solution for wave speed, $V(\phi_t, \sigma_t)$, as expressed by Eqs. (35) and (38).

Appendix B ENERGY CONSERVATION

Previous investigators^{37,38} have attempted to derive scaling relationships using energy conservation. We note here a potential fallacy in such an approach, show how to avoid it, and derive an upper limit for the wave velocity that is more general and yet consistent with the results presented earlier.

The power supplied by the electrode goes into field energy and gas dynamics according to

$$I_0 \phi_0 = V \left(\frac{1}{2} C_z \phi_0^2 + \frac{1}{2} L_z I_0^2 + \epsilon_f \right) \quad (\text{B1})$$

where ϵ_f is the energy absorbed per unit length by the gas and where the electrode current

$$I_0 = V C_z \phi_0. \quad (\text{B2})$$

These equations reduce to

$$\epsilon_f = \frac{1}{2} C_z \phi_0^2 (1 - V^2 L_z C_z). \quad (\text{B3})$$

Note that $\epsilon_f \rightarrow 0$ as $V \rightarrow (L_z C_z)^{-1/2}$; i.e., all the energy is stored in the electromagnetic fields.

A certain fraction f of the absorbed energy ϵ_f goes into ionization, which suggests that the final wave conductance is given by

$$\Sigma_f = f e \mu_f \epsilon_f / W \quad (\text{B4})$$

where W is the gas ionization energy. The wave velocity can be expressed according to Eq. (28) by

$$V = E_f \Sigma_f / C_z \phi_0. \quad (\text{B5})$$

Hence,

$$V = \frac{1}{2} f \frac{e \phi_0}{W} \mu_f E_f (1 - V^2 L_z C_z). \quad (\text{B6})$$

The usefulness of Eq. (B6) depends upon the ability to estimate f . As we now show, the assumption of constant f is often invalid.

Integrating the electron continuity Eq. (24) from the electrode to the wave tip yields

$$\Sigma_f = \frac{1}{V + \mu_f E_f} \int dz \bar{S} \Sigma \frac{\mu_f}{\mu} \quad (\text{B7})$$

where we have ignored the initial conductance, Σ_i , in comparison with Σ_f . To relate this to the energy absorbed by the gas, we note that the wave absorbs energy in the electron drift frame at a rate ΣE^2 . Transforming to the lab frame, the wave absorbs energy at a rate

$$\frac{\partial}{\partial t} \epsilon = \Sigma E^2 \frac{V}{V + \mu E} \quad (\text{B8})$$

where the final energy absorbed is given by

$$\epsilon_f = \int dt \frac{\partial}{\partial t} \epsilon = \int dz \frac{\Sigma E^2}{V + \mu E}. \quad (\text{B9})$$

We may thus rewrite Eq. (B7) as

$$\Sigma_r = \left\langle \frac{\bar{S}}{E^2} \left[\frac{\mu_r}{\mu} \right] \right\rangle \epsilon_r \quad (\text{B10})$$

where the average value of a variable x is defined by

$$\langle x \rangle = \frac{1}{\epsilon_r} \int dt \left[\frac{V + \mu E}{V + \mu_r E_r} \right] x \frac{\partial \epsilon}{\partial t} \quad (\text{B11})$$

Note that terms in parentheses are ~ 1 .

Comparison of Eqs. (B4) and (B10) leads to

$$f = \left\langle \frac{\bar{S}W}{e\mu E^2} \right\rangle \quad (\text{B12})$$

which re-expresses energy conservation. Wave velocity is thus given by

$$V = \frac{1}{2} \mu_r E_r \phi_0 \left\langle \frac{\bar{S}}{\mu E^2} \right\rangle (1 - V^2 L_z C_z) \quad (\text{B13})$$

To estimate f we rewrite Eq. (B12) in terms of the Townsend coefficients α and η :

$$f = \left\langle \frac{\alpha - \eta}{eE} W \right\rangle \quad (\text{B14})$$

Figure 5 shows a plot of the fraction

$$f' = \frac{\alpha - \eta}{eE} W \quad (\text{B15})$$

for weakly ionized air. This plot assumes an effective ionization energy of $W = 15$ eV, which equals the sum of the ionization potential plus the average kinetic energy of the plasma electrons. The strong dependence of f' on field parameter E/N demonstrates the fallacy of assuming constant f .

Equation (B6) can be used to provide an upper limit for wave speed V by noting that the ionization fraction

$$f < 1 \quad (\text{B16})$$

Using typical values for the downstream drift speed,

$$\mu_r E_r \leq 10^7 \text{ cm/sec} \quad (\text{B17})$$

and for the ionization energy,

$$W \geq 10 \text{ eV} \quad (\text{B18})$$

thus suggests that

$$V/\phi_0 < 5 \times 10^5 \text{ cm/Volt-sec} \quad (\text{B19})$$

irrespective of initial conditions, gas density, or wave propagation mechanism. This condition can be violated only if the average applied field appreciably exceeds the maintenance field E_r , or if the potential wave is nonionizing.

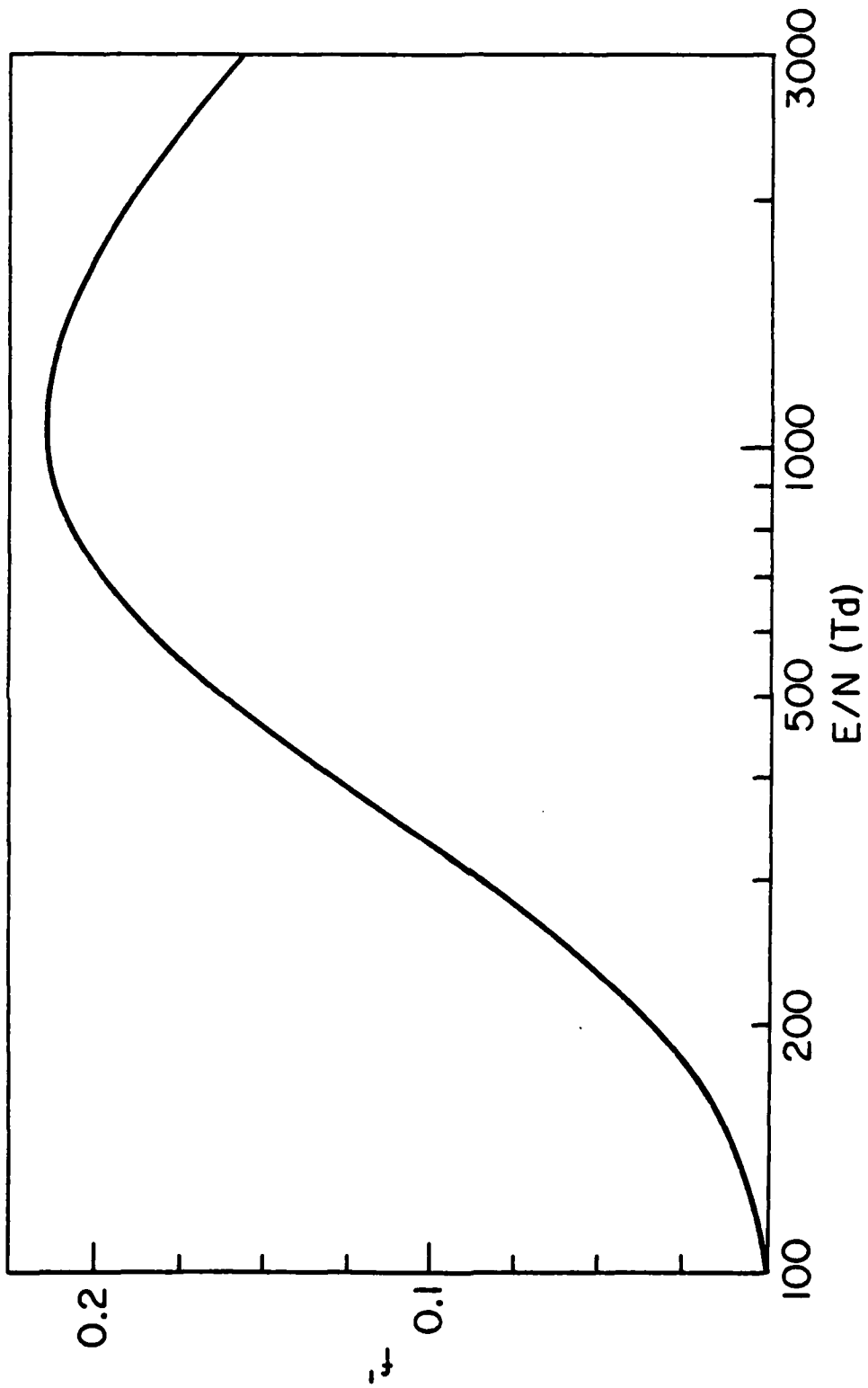


Fig. 5 — Fraction of energy going into ionization as a function of field strength in weakly ionized air at density N